nature physics

SUPPLEMENTARY INFORMATION

DOI: 10.1038/NPHYS4025

In the format provided by the authors and unedited.

Confined dense circumstellar material surrounding a regular type II supernova

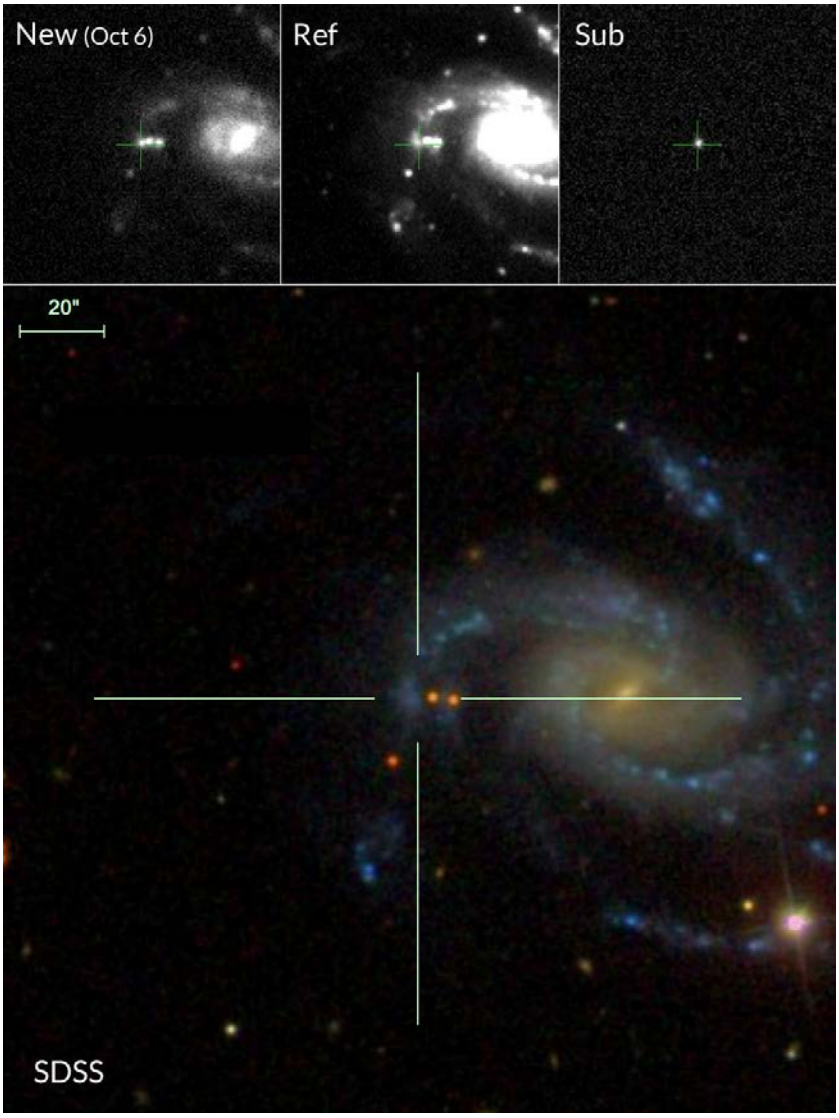

Supplementary Figure 1 Discovery of iPTF 13dqy in the nearby galaxy NGC 7610 ($d = 50.95$ Mpc), at $\alpha = 23^h19^m44.70^s$, $\delta = +10°11'04.4''$ (J2000.0). Top: Palomar 48-inch sequence of the new discovery image from 2013 Oct. 06.24, a reference image (a coadd of pre-explosion images), and the subtraction image. Bottom: The colour SDSS image. The SN is located in a blue, star-forming area (the red point sources in the vicinity are foreground stars), which is apparently a part of one of the major arms of the spiral host.

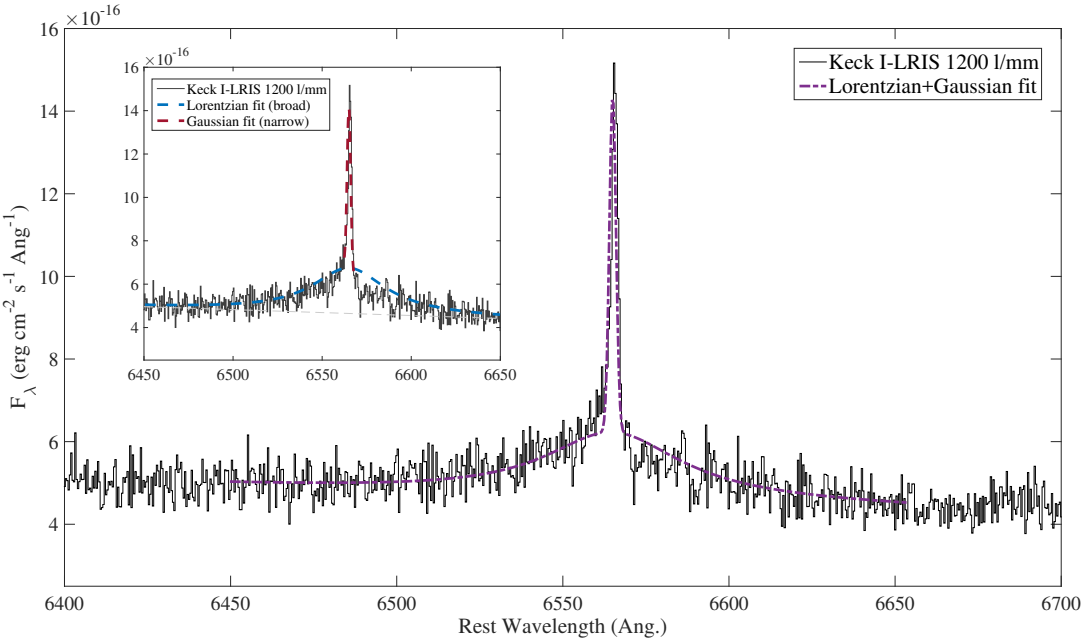

Supplementary Figure 2 Composite Gaussian and Lorentzian fits to the narrow and broad components of the Hα line in the Keck-I/LRIS 1200 lines mm^{-1} spectrum obtained ~ 10.3 hr after explosion. The FWHM of the narrow Gaussian fit is ~ 2.35 Å, corresponding to a wind velocity of $v_{\rm wind} \approx 100$ km s^{-1}. The instrumental resolution is around this velocity (LRIS manual, and verified from night-sky lines), so the line should be regarded as barely resolved, and the velocity estimate should be taken as an approximate close upper limit. The FWHM of the underlying broad wings, which we relate to electron scattering, is ~ 25 Å. The inset displays separate Lorentzian and Gaussian fits to the two components, focusing on the possible asymmetry of the line profile, especially a potential lack of flux on the red side.

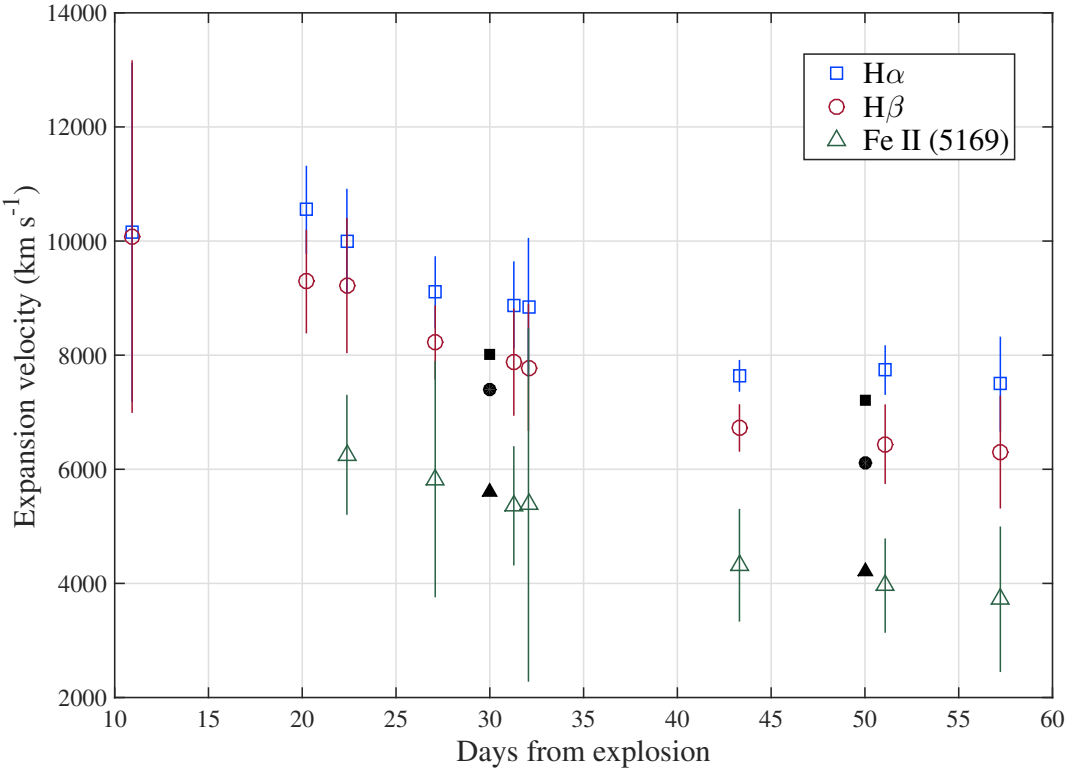

Supplementary Figure 3 Evolution of the expansion velocity of the SN ejecta for selected lines, between days 10 and 57 after explosion. The derived expansion velocities (and the uncertainties) were obtained by fitting a parabola to the minima of the P-Cygni absorption features. The Hα and Hβ lines evolve from velocities around $10,000$ to ~ 7000 km s^{-1} during this time interval, whereas the velocity of the Fe II $\lambda 5169$ line, visible from day 22 onward, decreases from around 6000 to $\lesssim 4000$ km s^{-1} by day 57. Overplotted with filled black markers are the expansion velocities (for the three lines: Hα, Hβ, and an average of Fe II lines) of the standard Type II-P SN 2004et at days 30 and 50, as presented by Ref. [62]. The obtained trend and values of the expansion velocities are in broad agreement with typical SNe II-P[17,18].

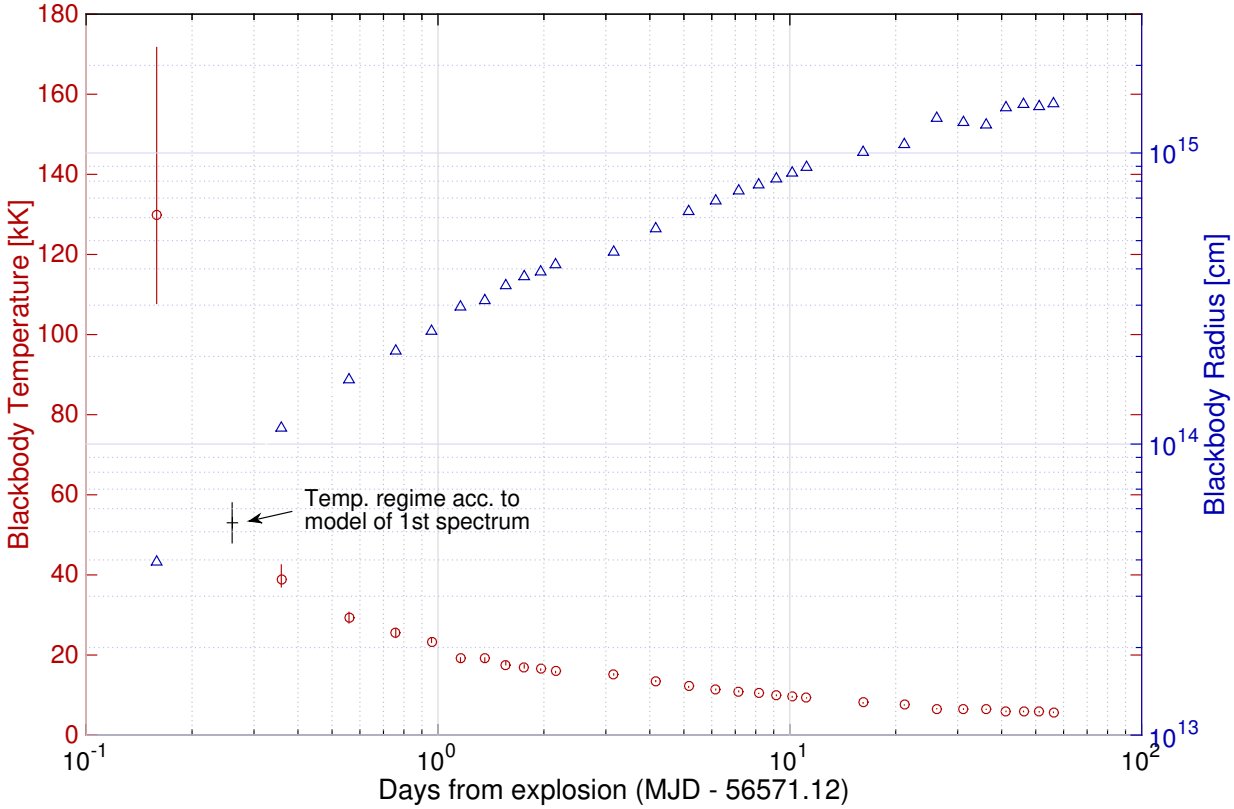

Supplementary Figure 4 Evolution of the estimated BB temperature and radius over the first 60 d after explosion, based on the multiband photometry measurements (Fig. 1). The first BB temperature estimate was obtained via careful extrapolation of the UVOT $UVM2$ and P60 $g+i$ light curves back to the first P48 (detection) point (see inset of Fig. 1 and text for details). The early-time BB temperature estimates, within the first half day after explosion, are also in agreement with our temperature estimates from the modeling of the early Keck spectra (Fig. 4), showing the highly ionised emission lines at temperatures $\gtrsim 50$ kK.

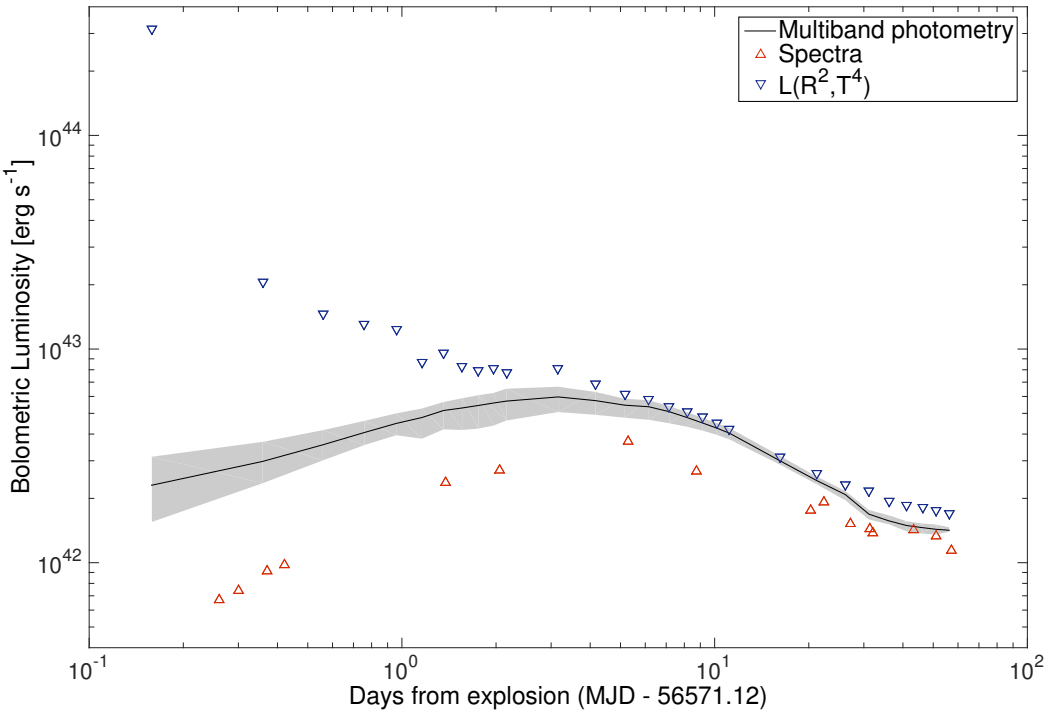

Supplementary Figure 5 Bolometric luminosity estimates over the first 60 d after explosion. The shaded region and the solid black line (a running mean of the region) denote bolometric luminosity estimates based on the multiband photometry (Fig. 1) according to three methods used to calculate the total flux from the SED: interpolation, order-4 polynomial fit, and BB fits. The top end of the shaded region can be regarded as our best lower limit on the real bolometric luminosity, based on the photometric observations. The red triangles denote a (more conservative) lower limit on the bolometric luminosity obtained from our spectra (Fig. 2, Fig. 3), beginning with the early set of 4 Keck spectra at $\lesssim 10$ hr after explosion and ending with our latest spectrum at 57.2 days. The blue triangles show the luminosity as obtained by our best BB temperature and radius estimates (Fig. 4), $L = 4\pi R^2 \sigma T^4$; the luminosity in the first point, at ~ 3.8 hr after explosion, exceeds $10^{44}\,\mathrm{erg\,s^{-1}}$.

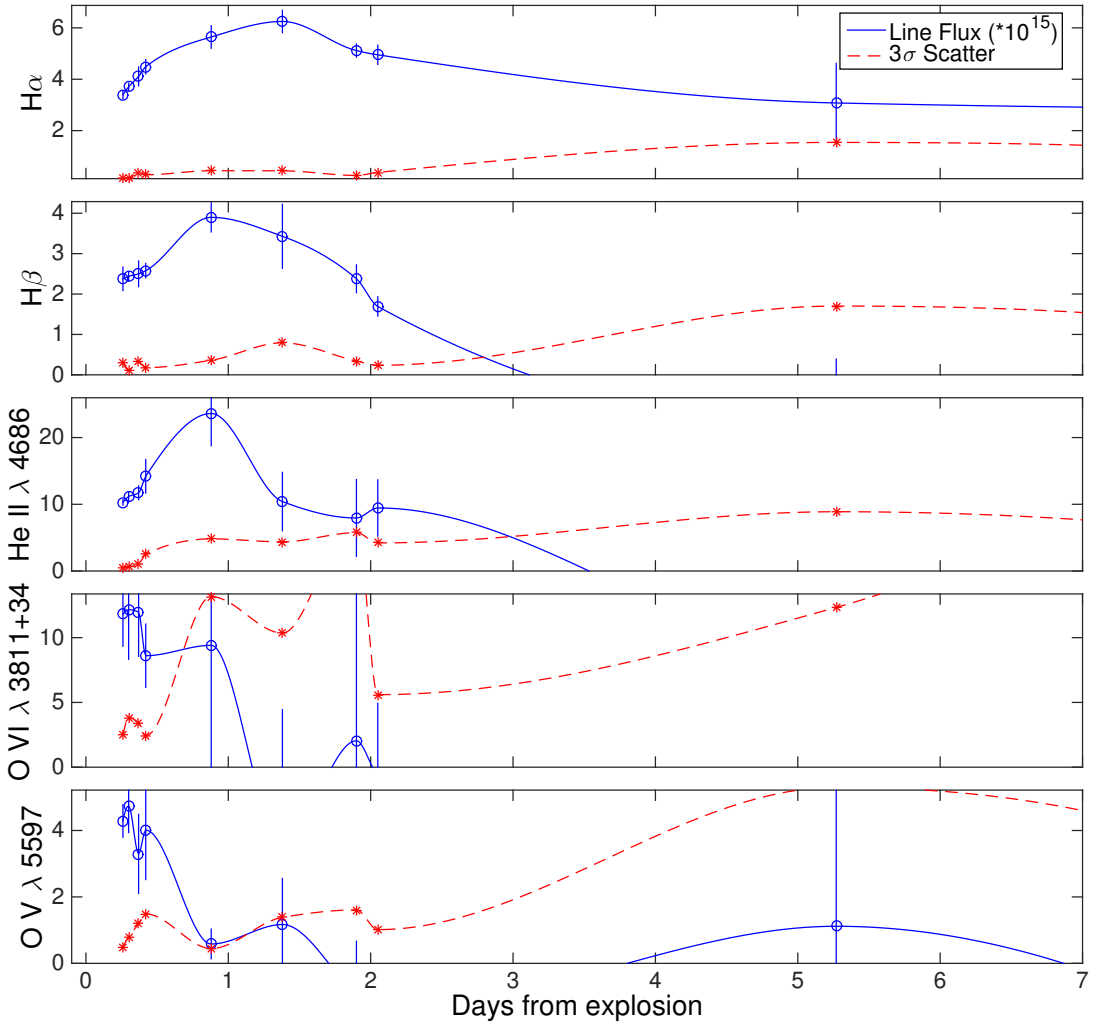

Supplementary Figure 6 Emission-line flux evolution during the first week after explosion. A 3σ uncertainty estimate based on the scatter is also plotted. Note the general shape of the Hα, Hβ, and He II emission-line flux curves, increasing and declining during the first ~ 2 d, whereas the highly ionised oxygen lines disappear completely (quickly falling to the background scatter) well within the first day after explosion.

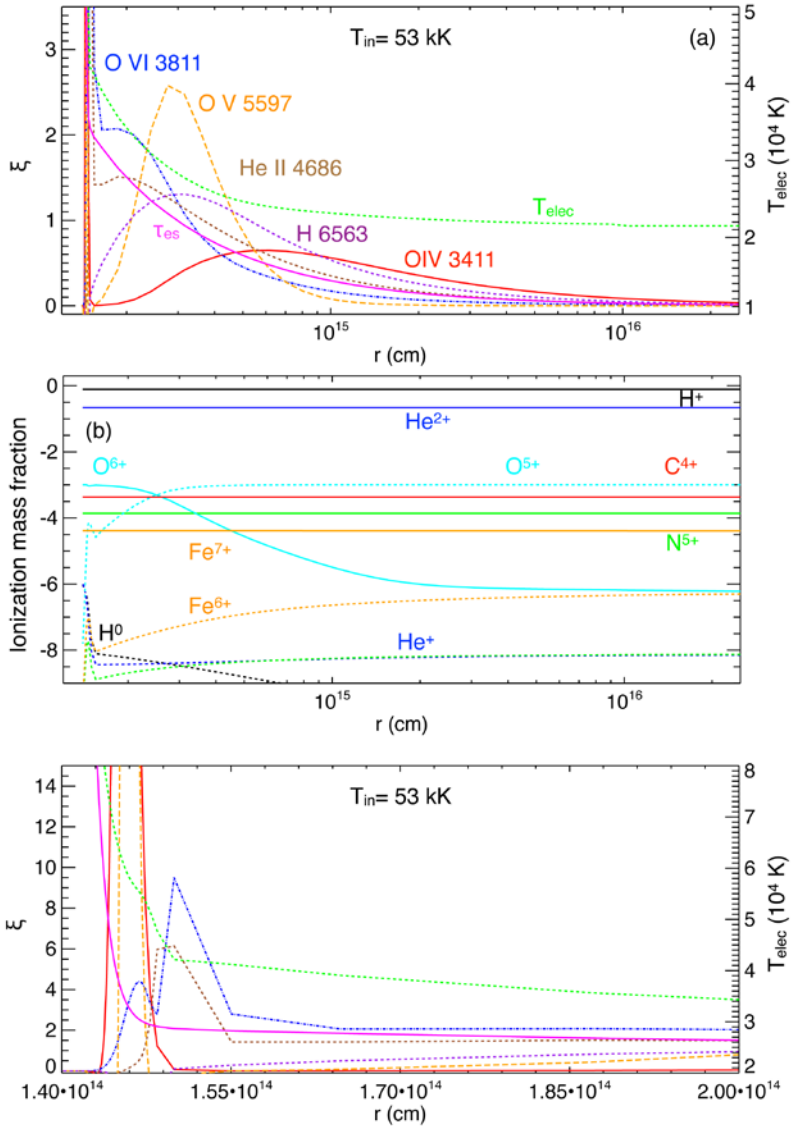

Supplementary Figure 7 Line-forming regions (top and bottom panels) and ionisation structure (middle) of the 53 kK model, fitting the 6 hr spectrum. The quantity ξ is related to the equivalent width of the line (following Ref. [63]) as EW $= \int_{R_{\rm in}}^{\infty} \xi(r) d(\log r)$. The bottom panel shows a close-up view of the very inner region, around $R_{\rm in}$ (colour coding is identical to the top panel.) Radial profiles of the electron optical depth and electron temperatures are shown in the top panel.

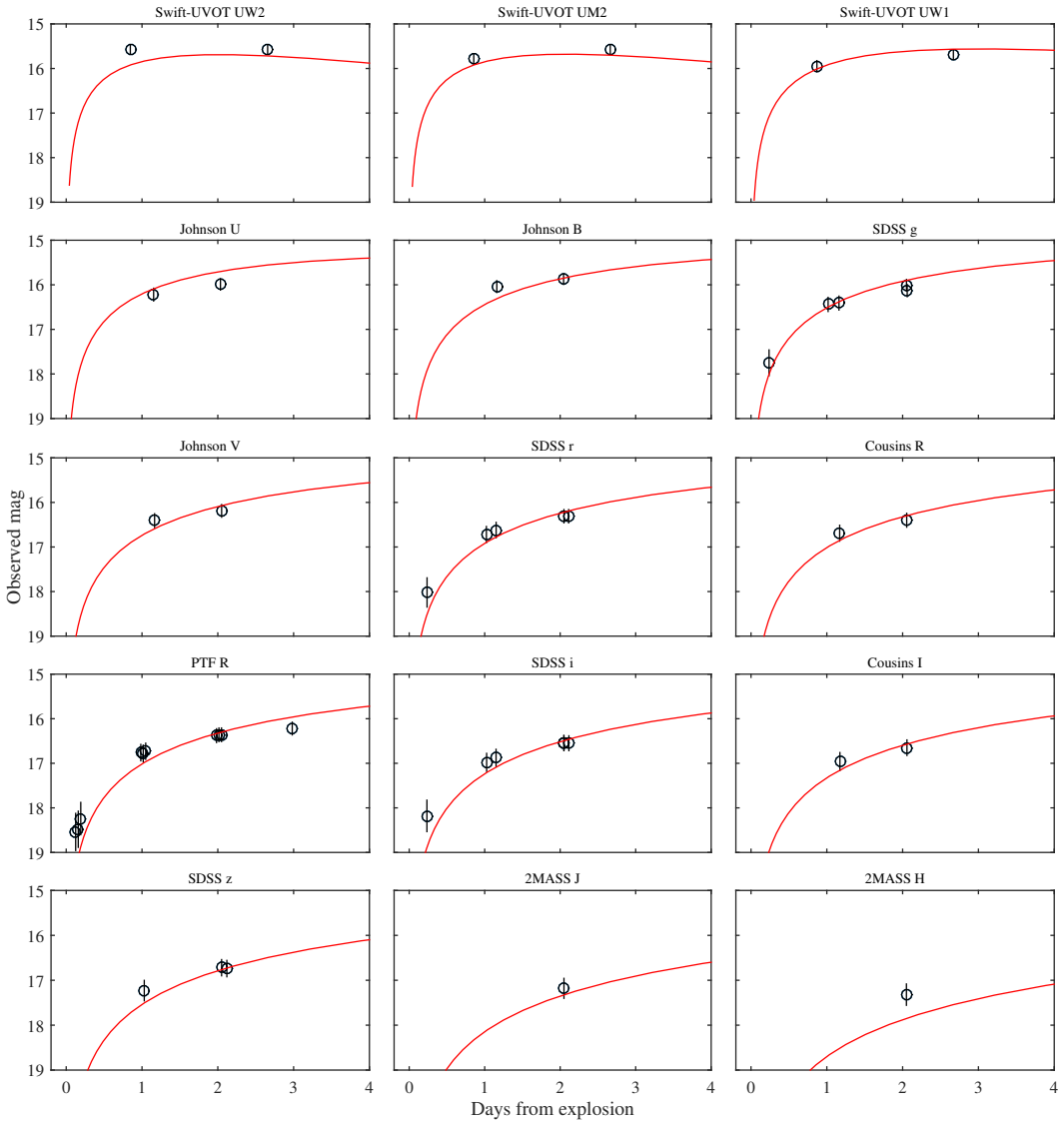

Supplementary Figure 8 Multicolour fits of RW11[23] models to the early-time photometry. The uncertainties have been scaled such that the minimal χ^2 per degree of freedom equals 1 (and the original relative errors in between measurements are maintained). See Ref. [24], presenting R-band fits of RW11 for a large sample of SNe II from the PTF and iPTF surveys.

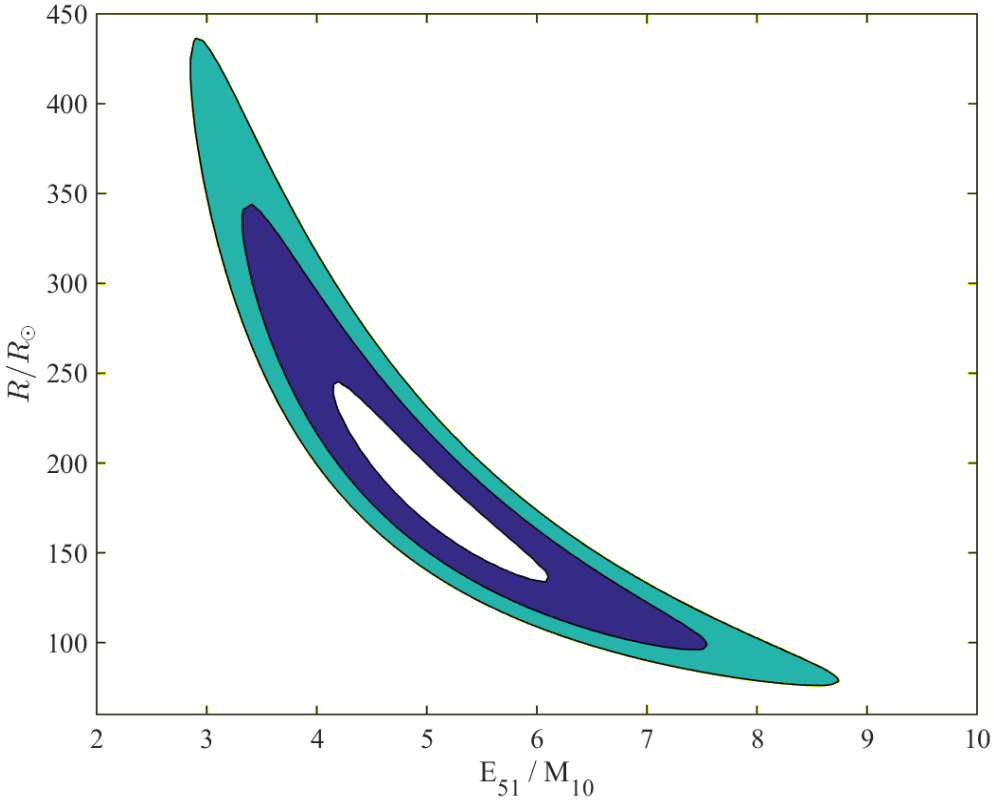

Supplementary Figure 9 Analysis of our multicolour UVOIR early-time data using the methods of Ref. [23] constrains the progenitor radius and explosion energy per unit mass. $1, 2, 3\sigma$ contours are plotted, as derived from χ^2 fits to all the data (see Ref. [24] for details).

UTC Obs-Date	Obs-Time	MJD	Phase[a]	Telescope/Instrument	Observer/Reducer
2013-10-06	09:10:36	56571.3824	6.2 hr	Keck-I/LRIS	D. Perley / D. Perley
2013-10-06	10:00:46	56571.4172	7.2 hr	Keck-I/LRIS	D. Perley / D. Perley
2013-10-06	11:39:05	56571.4855	8.9 hr	Keck-I/LRIS	D. Perley / D. Perley
2013-10-06	13:04:19	56571.5447	10.1 hr	Keck-I/LRIS	D. Perley / D. Perley
2013-10-06	13:13:49	56571.5513	10.3 hr	Keck-I/LRIS (Hi-Res)	D. Perley / D. Perley
2013-10-07	00:02:18	56572.0016	21.1 hr	NOT/ALFOSC	N. E. Groeneboom / F. Taddia
2013-10-07	12:06:39	56572.5046	1.4 d	FTS/FLOYDS	D. Sand / S. Valenti
2013-10-08	00:21:53	56573.0152	1.9 d	NOT/ALFOSC	N. E. Groeneboom / F. Taddia
2013-10-08	04:00:46	56573.1672	2.0 d	P200/DBSP	Y. Cao / Y. Cao
2013-10-08	06:34:07	56573.2737	2.1 d	Keck-II/DEIMOS	K. Clubb, M. Graham / P. Kelly
2013-10-11	04:48:12	56576.2001	5.1 d	Keck-II/DEIMOS	S. Tang / Y. Cao
2013-10-11	09:19:19	56576.3884	5.3 d	FTS/FLOYDS	D. Sand / I. Arcavi, S. Valenti
2013-10-14	21:05:02	56579.8785	8.8 d	WHT/ISIS	WHT service / K. Maguire
2013-10-17	01:10:33	56582.0497	10.9 d	NOT/ALFOSC	A. A. Djupvik / F. Taddia
2013-10-26	08:06:13	56591.3377	20.2 d	Lick-3 m/Kast	I. Shivvers, J. C. Mauerhan / S. B. Cenko
2013-10-28	12:05:01	56593.5035	22.4 d	FTS/FLOYDS	S. Valenti / S. Valenti
2013-11-02	04:59:51	56598.2082	27.1 d	P200/DBSP	A. Waszczak / P. Vreeswijk
2013-11-06	09:36:49	56602.4006	31.3 d	FTS/FLOYDS	S. Valenti / S. Valenti
2013-11-07	04:25:03	56603.1841	32.0 d	APO/DIS	M. Kasliwal / Y. Cao
2013-11-18	10:12:19	56614.4252	43.3 d	FTS/FLOYDS	S. Valenti / S. Valenti
2013-11-26	04:50:56	56622.2020	51.1 d	P200/DBSP	A. Waszczak / O. Yaron
2013-12-02	08:15:32	56628.3441	57.2 d	Keck-I/LRIS	Y. Cao, D. Perley / D. Perley

Supplementary Table 1 Log of Spectroscopy. Additional meta-data and the full set of spectra are publicly available through WISeREP (http://wiserep.weizmann.ac.il). Notes: [a]Hours/days with respect to the

estimated explosion time (at $\mathrm{MJD}_0 = 56571.12$).